Engineering Structures 132 (2017) 29–43

Contents lists available at ScienceDirect

Engineering Structures

journal homepage: www.elsevier.com/locate/engstruct

Incremental dynamic analysis with multi-modes for seismic performance evaluation of RC bridges

Prakit Chomchuen *, Virote Boonyapinyo

Department of Civil Engineering, Faculty of Engineering, Thammasat University, Rangsit Campus, Klong Luang, Pathumthani 12120, Thailand

ARTICLE INFO

Article history:
Received 17 December 2014
Revised 8 November 2016
Accepted 11 November 2016
Available online 22 November 2016

Keywords:
Incremental dynamic analysis
Multi-mode combination load pattern
Pushover analysis
Seismic performance evaluation
Reinforced concrete bridge

ABSTRACT

This study aimed to investigate the seismic performance of the typical single column reinforced concrete bridges in Thailand under the earthquake intensity level of Bangkok by the mean of incremental dynamic analysis (IDA). The concept of IDA by equivalent single-degree-of-freedom system (ESDOF) was adopted to evaluate the seismic performance of the studied bridges by the charms of less computational price. The effects of two important parameters that influence the seismic behavior generated by the IDA of ESDOF, i.e. lateral load pattern and hysteresis model, were also investigated. The results show that the different load patterns result in significantly different seismic behavior, especially for the bridge with low participating mass ratio for fundamental mode, while the using of different hysteresis models show less significance. The simple standard-based load patterns can be used effectively only for the bridge which is dominated by the fundamental mode. To account for the higher mode effects, but retain the simplicity of single-run nonlinear static analysis (NSA) and nonlinear time history analysis (NTHA) of ESDOF, the multi-modes combination load pattern is proposed in this study. The distribution of load can be generated by the simple combination of considered mode shapes weighted by their modal participating mass ratios. By using the proposed load pattern, the seismic behavior evaluated by the IDA of ESDOF agree well with the results of IDA of multi-degree-of-freedom system for all studied bridges. The results also show that the studied bridges can resist the considered earthquakes without any damage.

© 2016 Elsevier Ltd. All rights reserved.

1. Introduction

Nonlinear time history analyses (NTHA) of structures under monotonically scaling up considered ground motion until the response of structure shows collapse is the key concept of Incremental Dynamic Analysis (IDA) that has been compiled and proposed by [1]. The monotonic scalable ground motion intensity measure (IM) was plotted together with a damage measure (DM) called incremental dynamic analysis curve (IDA curve). The IDA curve contains the necessary information to assess the performance levels or limit-states of the structures that are important ingredients of Performance Based Earthquake Engineering (PBEE). The IDA attracts the researchers and engineers to use as the tool for evaluating the seismic behavior of the structures [2–7].

To reduce the computational price and time of using NTHA of multi-degree of freedom structures (MDOF), the concept of equivalent single-degree of freedom (ESDOF) has been investigated [8]. The lateral behavior of MDOF under the lateral force is evaluated by the Nonlinear Static Analysis (NSA) and apply to be the equivalent behavior of the Single-Degree-of-Freedom system. Then, the lower computational price of NTHA of ESDOF will be performed to evaluate the IDA curve. Vamvatsikos and Cornell [9] proposed the empirical correlation between the standard pushover curves and IDA curves. FEMA P440A [10] investigates the effect of stiffness and strength degradation on the seismic response of structures by using concept of ESDOF. Because of using the result of the NSA to be the lateral behavior of the ESDOF, the drawback of the standard NSA has remained in the IDA results, i.e. the effect of higher mode of vibration is not included in the standard NSA. To account the higher mode effect, several advance IDAs have been proposed [11–14].

There are several methods that have been proposed to account the higher mode effect in the NSA, e.g. Modal Pushover Analysis (MPA) [15], Energy-Based Pushover Analysis (EPA) [16], and Adaptive Pushover Analysis (APA) [17]. The MPA requires multiple analyses of NSA under various considered modal load patterns while EPA and APA require the experienced engineer who can interpret for using advanced computer programs, therefore, there are not an attractive proposition in engineering practice. Kunnath [18] has proposed the method to include the higher mode effect in

* Corresponding author.
E-mail addresses: cprakit@gmail.com (P. Chomchuen), bvirote@engr.tu.ac.th (V. Boonyapinyo).

http://dx.doi.org/10.1016/j.engstruct.2016.11.026
0141-0296/© 2016 Elsevier Ltd. All rights reserved.

NSA by developing a new lateral load configuration using factored modal combinations. The higher modes contribution were accounted in the lateral load pattern and the single-run NSA is required by this method. The literature also shows that numerous limitations exist depending on the modal response of the structural system and failure mode types, e.g. Del Vecchio et al. [19].

Bridge is an important structure. Then, many researchers investigate the seismic performance of this type of structure [20–26]. Both conventional and advanced NSA are used as the tool for evaluating the seismic performance of the bridge structures. Mander et al. [2] use the IDA to assess the seismic financial risk of bridges. The literature shows that even if the IDA by ESDOF of the building structures have been widely investigated, this concept for the bridge structures is few and not yet clearly explained.

The single-column bridges are generally weak under earthquake because the large mass of the superstructure is supported by the single column as seen from the damage of this bridge type in the Kobe earthquake [27]. This kind of bridge was widely used in Bangkok, the capital city of Thailand. The oldest one is the part of the expressway, the main line of transportation. It was constructed in 1979 without seismic details. Department of Public Work and Town & Country Planing of Thailand has announced the seismic design standard for the seismic risk regions in Thailand in 2009 [28]. Bangkok is classified as low to moderate seismic risk region. Therefore, the seismic behavior of this bridge type should be evaluated.

Therefore, this paper has two principal objectives. First is to present the technique that retains the simplicity of single-run analysis for performing IDA of ESDOF of the flexible structure like bridges. A lateral load pattern that includes higher mode effect for single-run displacement-based NSA to evaluate the lateral behavior of ESDOF is proposed in this study. Efficiency of proposed technique is investigated through the intensive investigation of applicability of IDA of ESDOF with proposed load pattern in evaluating seismic performance of single column RC with three different column heights. Second is to evaluate the seismic performance of the typically single-column reinforced concrete bridge used in Thailand.

2. Case study of single-column RC bridge structures

This study investigates a single column reinforced concrete bridge as case study because this bridge type is weak under earthquake because the massive mass of the superstructure is supported by only single-column. The single column bridges are typically used in Thailand as shown in Fig. 1(a). Three different column heights of studied bridge are considered in this study, i.e. 4.5 m, 6.3 m, and 15.0 m, as shown in Fig. 1(b), in order to investigate the effects of column flexibility on the seismic performance of the studied bridge and efficiency of the proposed evaluation methods. Furthermore, fundamental frequency of studied bridges are evaluated and then compared with the field test data.

2.1. General configurations and analytical model

The studied bridges are single column reinforced concrete bridge of expressway phase 1 since 1976 in Bangkok, Thailand. A specification describing a bridge in detail is referred to as its as-built drawing. The design strengths of concrete are 23.54 MPa and 34.32 MPa for in-situ reinforced concrete and precast prestressed concrete beam, respectively. The grade 40 deformed bar, with a yield strength and ultimate strength equal to 392.27 MPa and 558.98 MPa respectively, was used for reinforcement. Components of the studied bridges are divided into four components, i.e. superstructure, bearing system, substructure and foundation. Details of each component are described as follows except foundation. The foundation system of the studied bridges is 4.80 m × 6.60 m × 1.40 m reinforced concrete footing sitting on 10-∅0.60 m prestressed concrete piles. This paper considers that the foundation system is stronger than other component under lateral excitation. Accompany with the main objective of this paper is to study the efficiency of ESODF concept for evaluating the seismic performance of single column RC bridge by comparing with MDOF concept, therefore, the foundation of studied bridges is assumed to be fixed support for all case studies. Although considering the effects of soil-structure interaction may lead to more flexible structural system, the fixed support that assumed in this paper will suffice to reflect the effects of studied parameters.

2.1.1. Superstructure

The superstructure of the studied bridges is an 18-cm-thick reinforced concrete slab placed on the top of five pre-stressed concrete I-girders as shown in Fig. 2. It is assumed to be elastic and modeled by lumped single elastic beam-column elements. According to the bridges modeling for nonlinear analysis proposed by Aviram et al. [29], four elements per span are used in this study. The translational mass of the superstructure is automatically calculated and lumped to the nodes of beam-column element. Torsional mass, which affects to the dynamic properties of the bridges especially in transverse direction, is also calculated and defined to the nodes of elements manually.

2.1.2. Bearing system

Bearing system of the studied bridges is the bearing pad system as shown in Fig. 3(a). It is modeled by elastic six degree-of-freedoms spring element. Three of the six degree-of-freedoms of spring element is shown in Fig. 3(b). The stiffness of each degree of freedom is calculated by the beam theory suggested by Yazdani et al. [30]. The shear modulus of the rubber depends on its hardness. The report of Thammasat University Research and Consultancy Institute (TU-RAC) [31] about the inspection of bearing pads of the expressway in Bangkok shows that the hardness of the bearing pad's rubber is about 60 Shore A scale. AASHTO [32] suggests that an appropriate shear modulus of the rubber with 60 Shore A scale is 0.9 MPa. Although the effective compressive modulus of elasticity of the new bearing pads can be calculated directly from specified shear modulus according to the method in AASHTO [32], Yazdani et al. [30] have shown that aging and cold temperature elastomers may experience significant stiffening. The increase in stiffness may be as high as 50 times the original stiffness. The stiffness of bearing pad in this study are summarized in Table 1.

2.1.3. Substructure

The substructure system of the studied bridges is an octagon cross-section reinforced concrete column with a top slab. The cross-section of the column is 1.60 × 1.60 m as shown in Fig. 4(a). The bottom of the bridge columns are modeled by the inelastic element in order to capture the inelastic behavior of the bridge structures. For nonlinear static analysis, the inelastic behavior is modeled using the lumped hinge technique. The lumped axial-bidirectional moment interaction hinge (P-M-M) is used in this study. An example of moment-curvature of the specified column cross-section is shown in Fig. 4(b). The column reaches the limit when the extreme fiber of the cross-section reaches the ultimate compressive strain. When the column is subjected to an axial load, the moment-curvature is adjusted automatically by considering the interaction diagram shown in Fig. 4(c).

Due to a limitation of SAP2000, the plastic hinge length element with lumped hinge is replaced by a nonlinear spring element to model the inelastic behavior of the bridges for NTHA. The

(a) Various application of single column RC bridges in Bangkok, Thailand

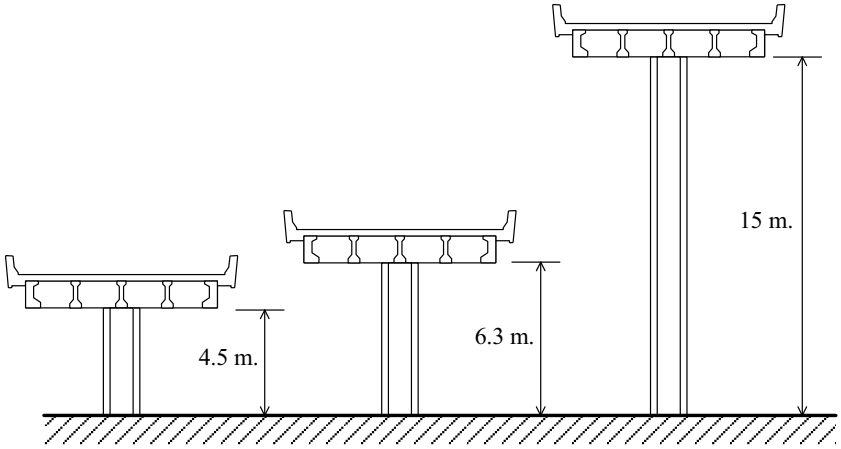

(b) Studied bridge with three different column heights

Fig. 1. General configurations of studied single column reinforced concrete bridges.

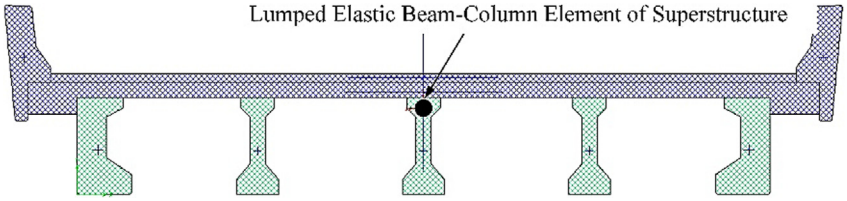

Fig. 2. Superstructure of the studied bridges.

moment-curvature of the column cross-section of all studied bridges, which are evaluated taking into account the interaction with axial load, are defined to the nonlinear spring element in nonlinear time history analytical model. The fundamental natural frequency of the nonlinear time history analytical model are compared to those of the nonlinear static analytical model to make sure that the dynamic properties of both models are the same by comparisons of load-displacement curves of both models.

The top of the column is rigidly connected to the 1.33-m-thick cast-in-place reinforced concrete slab (Fig. 4(d)). It is modeled as an elastic thick shell element. This element is used to realistically model the mass distribution of the slab. Because of the high thickness-to-width ratio of the slab, a thick element was used to account for the influence of shear deformation.

Gap element is used to model the gap between superstructure and substructure. The initial gap was set to 2 cm as same as the

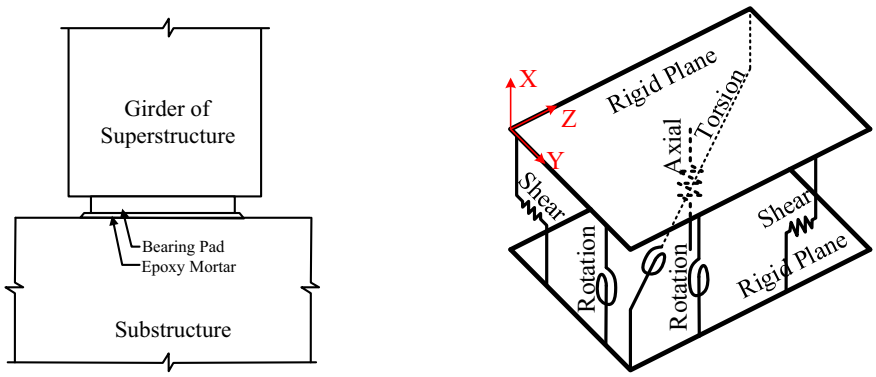

(a) Bearing pad of the bridge (b) Six degree of freedom spring element

Fig. 3. Bearing system modeling.

Table 1
Stiffness of bearing pad in six directions.

Axial stiffness (K_X) (kN/mm)	Shear stiffness in Y direction (K_Y) (kN/mm)	Shear stiffness in Z direction (K_Z) (kN/mm)	Torsional stiffness about X (K_{RX}) (kN-mm/rad)	Rotational stiffness about Y (K_{RY}) (kN-mm/rad)	Rotational stiffness about Z (K_{RZ}) (kN-mm/rad)
35,635.19	64.8	64.8	2.093e+6	1.105e+6	489.5e+6

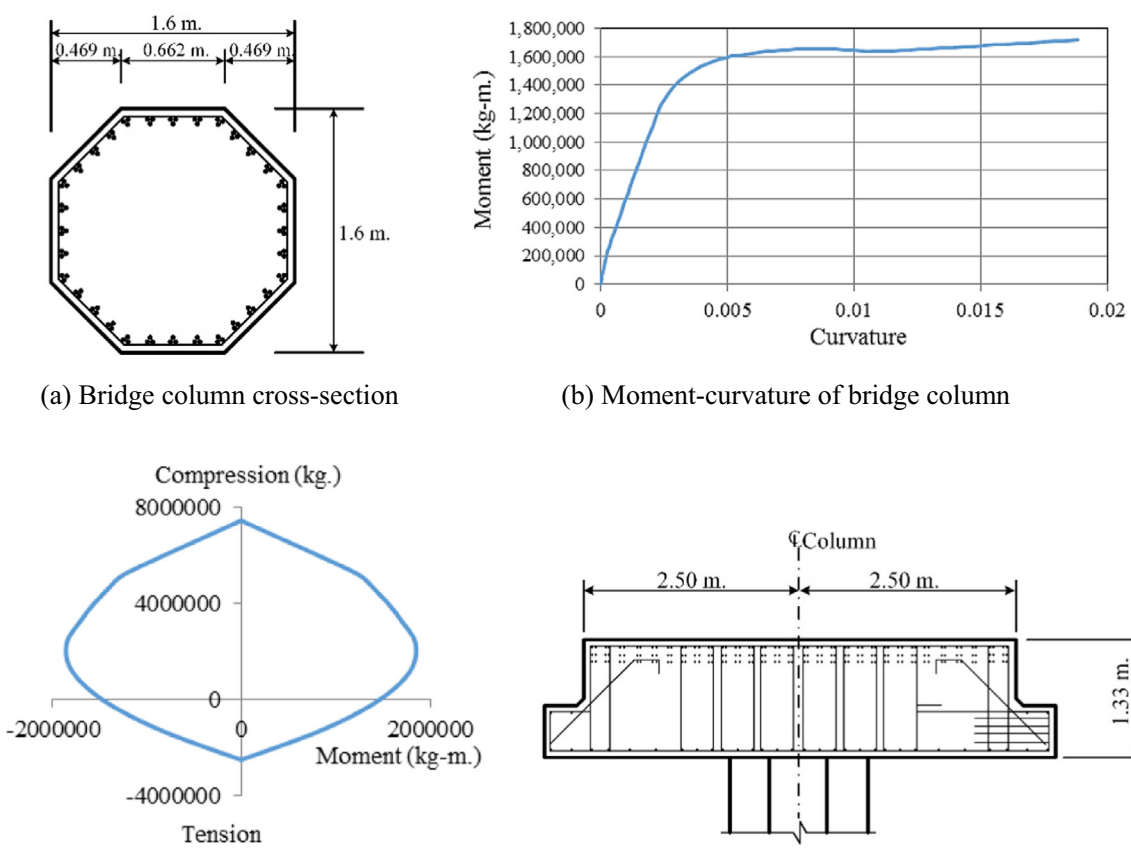

(a) Bridge column cross-section (b) Moment-curvature of bridge column

(c) Interaction Diagram (d) Slab at the top of bridge's column

Fig. 4. Details of substructure properties.

detail of as-built drawing. To avoid the rounded-error, the stiffness of the gap element is about 100 times of axial stiffness of the superstructure [33].

According to the modeling concepts described above, Fig. 5(a) shows the summary details of the bridge components modeling. The MDOF analytical model of the studied bridge is shown in Fig. 5(b).

2.2. Dynamic properties of studied bridges

The dynamic properties of the studied bridges are assessed via the method of vibration mode finding analysis. Eigen-problem analyses of the provided analytical model of the bridges are performed to evaluate the mode shapes and frequencies of all studied bridges.

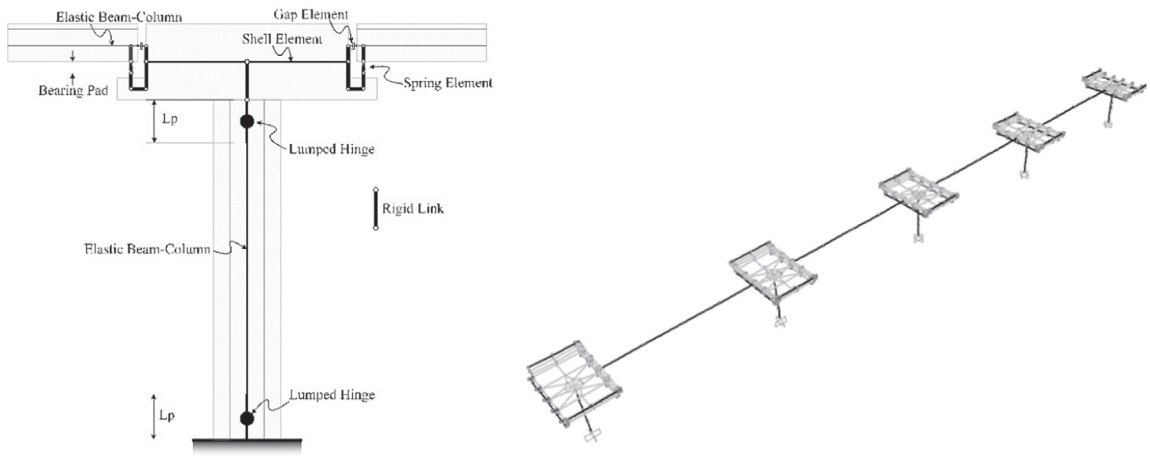

(a) Detail of each component modeling (b) Analytical Model in the computer program

Fig. 5. Analytical model of studied bridges.

The results show that the fundamental mode of vibration of the single column bridge is the oscillation of the structure in a direction perpendicular to the traffic direction so-called the transverse direction while the perpendicular direction so-called longitudinal direction. The fundamental mode shapes of the studied bridge in both directions are shown in Fig. 6(a) and 6(b), respectively. The dynamic properties of the studied bridges are concluded in Table 2.

To validate the analytical model, the calculated frequencies of a bridge with 6.3 m column height are compared to those from field test results. Due to the limitations of field test apparatus, the field test results are only shown in form of range of frequencies. The frequencies of the bridges in the transverse and the longitudinal directions of the field test are 1.60–2.00 Hz and 2.00–2.80 Hz, respectively. These numbers show that the calculated frequencies are in the range of the field test results. Therefore, the analytical model can be used to reliably evaluate the seismic performance.

The participating mass ratios of all bridges are also shown in Table 2. These results show that the vibration of a bridge with tall columns is dominated by the fundamental mode. Also, higher modes may be more influential when the bridge column height decreases.

According to the Seismic Retrofitting Manual for Highway Bridges published by the Federal Highway Administration in 2006 [34], the invisible crack in the structural member may affect the flexural rigidity of the members and should be considered in the seismic evaluation. This study also considered the effect of cracked sections in the seismic performance evaluation process. Then, the flexural rigidity of the reinforced concrete column of all studied bridges are reduced to half of that of the gross-section ($0.5E_cI_g$) in the process of seismic performance evaluation.

3. Seismic performance evaluation by incremental dynamic analysis

The evaluation seismic performance of the structures by IDA has two main tasks, which are evaluating seismic demand under set of ground motions by IDA and applying the capacity (limit state) to demand in order to evaluate probabilistic of damage of the structures.

3.1. IDA of multi-degree of freedom system

In conventional IDA, the NTHA of MDOF analytical model are performed under the set of monotonically increasing ground motions in order to investigate the seismic behavior of the structure under considered ground motion until collapse (seismic demand). The scalars that can reflect the intensity of ground motion called Intensity Measure (IM) are collected at every step of scaling-up considered ground motion. The maximum response of the structure which can reflect the damage level of the structure called Damage Measure (DM) also are collected corresponding with IM. Plotting IM together with DM is called incremental dynamic analysis curve (IDA curve) that indicates the seismic behavior of the structure from under the small ground motion to

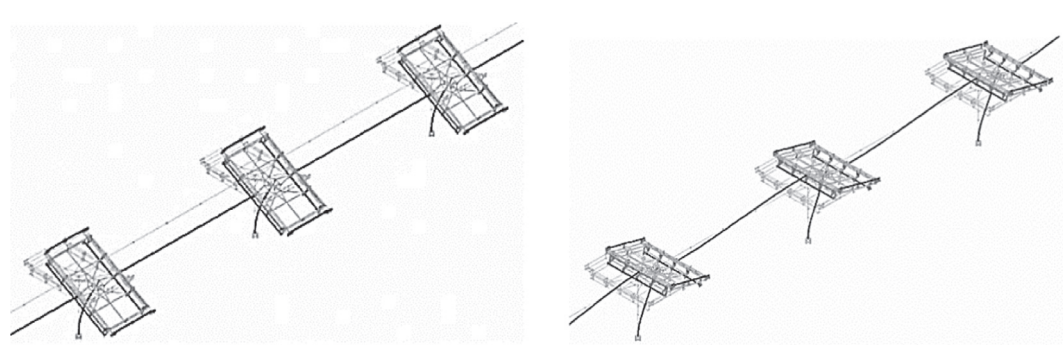

(a) Transverse mode shape (b) Longitudinal mode shape

Fig. 6. Fundamental mode of vibration of the studied bridges in transverse and longitudinal direction.

Table 2
Fundamental dynamic properties of vibration of three studied bridges.

Column height (m)	Transverse direction			Longitudinal direction		
	Period (sec)	Frequency (Hz)	Modal participating mass ratio (%)	Period (sec)	Frequency (Hz)	Modal participating mass ratio (%)
4.5	0.450	2.224	53.3	0.272	3.679	66.2
6.3	0.610	1.640	68.3	0.358	2.796	87.1
15.0	1.746	0.573	86.6	0.980	1.020	92.8

the largest one that make the structure collapse. Overview of performing IDA of MDOF of the studied bridges is shown in Fig. 7. This study use results of IDA of MDOF to be benchmark in evaluating efficiency of proposed technique.

3.2. IDA of ESDOF based on nonlinear static analysis

The concept of IDA based on nonlinear static analysis has been considered in order to reduce the computational price and time of IDA of MDOF [9]. The lateral behavior of the structure is generated by the nonlinear static analysis (NSA) under a suitable lateral load pattern. The cyclic nonlinear static analysis will be performed if the hysteresis behavior of the structures is required. Then, the generated lateral behavior is defined for the single degree of freedom system (SDOF) to be equivalent to that of the MDOF structure. The mass of SDOF is defined by a value that makes the fundamental dynamic properties of SDOF equal to the MDOF. An SDOF system that has lateral behavior equivalent to that of an MDOF system is used to perform the IDA. The concept of ESDOF is shown in Fig. 8. By using this method, the computational time can be significantly reduced [12]. Although advanced method for modal IDA has been proposed [12], that method requires IDA for each mode. The proposed method in this study applies a single-run analysis of NSA and IDA.

3.3. Lateral load pattern for single-run nonlinear static analysis

3.3.1. Conventional-based lateral load pattern

In evaluating the seismic behavior of structures using methods based on the NSA, international standards, such as FEMA 356 [35], suggest that at least two lateral load patterns should be considered. One of the load patterns can be selected from the following two categories.

The first category is the modal pattern. The distribution of vertical load can be selected from one of the following: The distribution proportional to the shape of the fundamental mode in the direction under consideration, and the distribution proportional to the story shear distribution calculated by combining modal responses from a response spectrum analysis of the building, including sufficient modes to capture at least 90% of the total building mass, and using the appropriate ground motion spectrum.

For the second pattern, the distribution can be selected from one of following: uniform distribution consisting of lateral forces at each level proportional to the total mass at each level (or uniform acceleration load distribution), and adaptive load distribution that changes as the structure is displaced.

This study applies the two lateral load patterns selected from the two categories above in order to investigate the effects of different lateral load patterns on the seismic behavior of single-

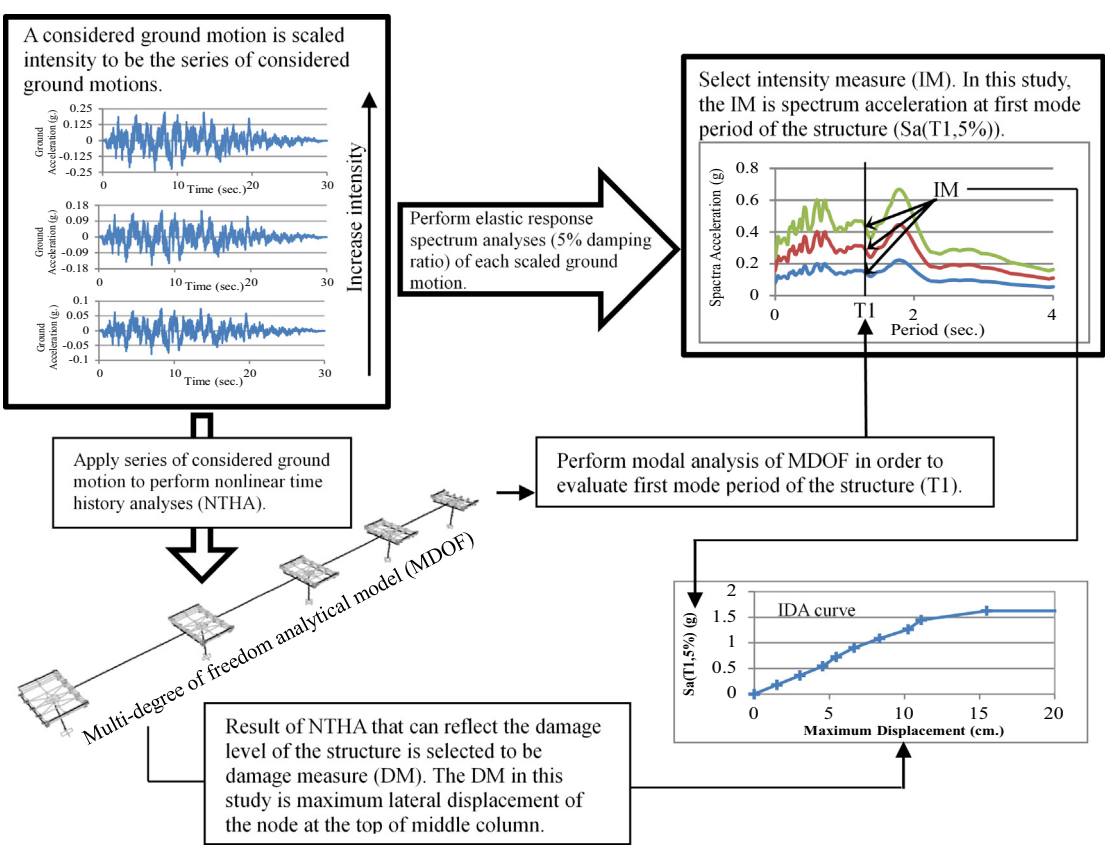

Fig. 7. Concept of incremental dynamic analysis of single column bridges.

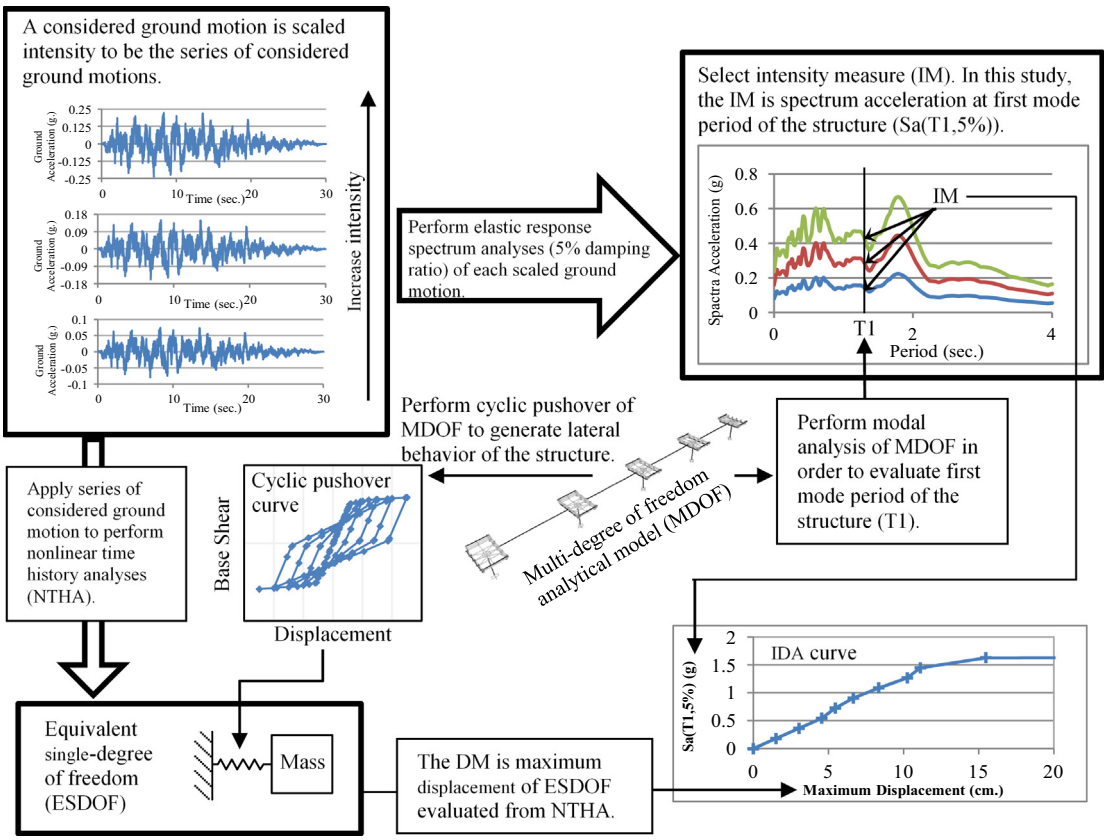

Fig. 8. Concept of incremental dynamic analysis by ESDOF based on nonlinear static analysis.

column RC bridges by using the concept of IDA of ESDOF. The first load pattern distributes the load proportionally to the fundamental mode in the transversal direction, referred as "First mode load pattern (1st)". The second load pattern is the uniform distribution consisting of lateral forces at each level proportional to the total mass at each level, referred as "Uniform acceleration load pattern (Unif)".

3.3.2. Proposed multi-modes combination load pattern

Multi-Modes Combination load pattern (MMC) is proposed in this study in order to account the higher mode effect, but retain the simplicity of single-run NSA and NTHA of ESDOF. The distribution of load can be generated by the simple combining of mode shapes which weighted by its modal participating mass ratios as follows:

$$F_j = \sum_{n=1}^{N} \Gamma_n \phi_{nj} \tag{1}$$

where F_j is the force at the j degree of freedom. Γ_n is the modal participating mass ratio of n mode. And ϕ_{nj} is the mode shape value at j degree of freedom of n mode which are each normalized with respect to the mass matrix such that $\phi_n^T M \phi_n = 1$. N is the number of consideration modes.

The proposed MMC gives only the distribution pattern of load that is used to perform the displacement-based NSA by the mean of SAP2000 in this study. The magnitude of load is monotonically increased until the displacement of the monitor point reaches the specified value by keeping the proportion of load the same as the specified load distribution. This method is similar to the method of mode combination proposed by Kunnath [18] for the force-based nonlinear static analysis. However, this study eliminates few parameters in order to make it more simple, but still accurate to use for the displacement-based nonlinear static analysis.

Mode shapes and participating mass ratios of each mode are shown in Table 3. To consider the higher modes for the MMC in this study, the four modes as shown in Table 3 are combined to capture at least 80% of the total mass for the studied bridges with short and medium column height. For the studied bridge with tall column height, the combination of four lateral modes was also applied.

3.3.3. Comparison of load patterns

According to the details described in Sections 3.3.1 and 3.3.2, the three studied load patterns for the studied bridge with 6.3 m column height are compared in Fig. 9. Fig. 9 shows that the Unif produces the smallest magnitude of resultant force. The 1st produces the largest magnitude of resultant force. The magnitude of resultant force of MMC is between those of Unif and 1st. It should be noted that the level of nodes of top slab and nodes of superstructure are different because the 1.33-m-thick cast-in-place reinforced concrete slab at the top of column is modeled by thick shell element at the middle of thickness of slab while the superstructure is modeled by elastic beam-column element at centroid of the section. Therefore, the level of superstructure is higher than the top slab of column as shown in Fig. 9(b).

3.4. Limit states of the studied bridges

The definition of the limit-state is the most important for evaluating seismic performance of the structures by IDA. There are several limit-states that can be defined on the IDA curve. Vamvatsikos and Cornell [1] applied the criteria of immediate occupancy (IO) and collapse prevention (CP) limit-states to their IDA for building. HAZUS [36] defines the qualitative definition of the limit states called damage states (DS) for the bridge structure by divided

Table 3
Mode shapes and participating mass ratios of three studied bridges in transverse direction for MMC.

Mode number	Mode shape	Participating mass ratio (%)		
		4.5 m column height	6.3 m column height	15 m column height
1		53.3	68.3	86.6
3	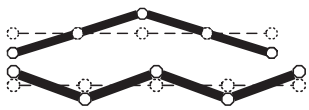	0.53	0.62	0.09
5		0.12	0.15	0.01
8		28.4	15	1

[a*] First mode of column.
[b*] Second mode of column.

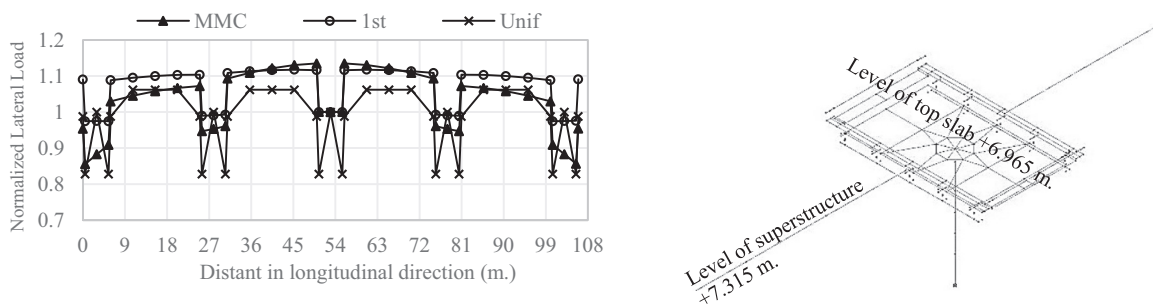

(a) Comparison of transverse load patterns (b) Different level of top slab and superstructure

Fig. 9. Comparison of three studied load patterns of the studied bridges with 4 spans and 6.3 m column height (see Fig. 5).

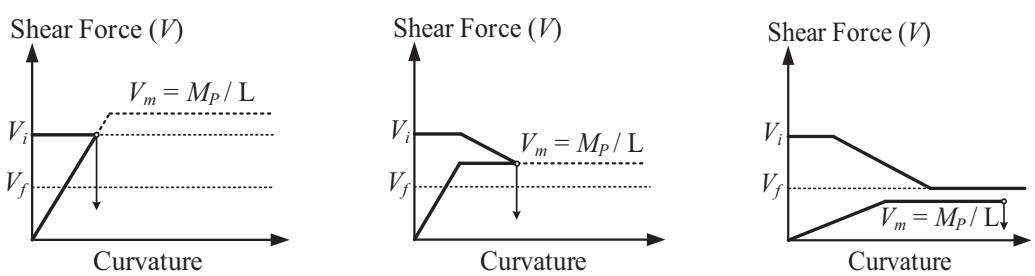

(a) Brittle failure (b) Semi-ductile failure (c) Flexural failure

Fig. 10. Possible failure mechanisms of bridge column with shear failure consideration according to FHWA.

into five states, i.e., none (DS1), minor/slight (DS2), moderate (DS3), major/extensive (DS4), and complete/collapse (DS5) damage states. Mander et al. [2] adopt the concept of DS and proposed that the quantity of each state can be extracted from pushover curve of bridge. Jeon et al. [26] suggested that the limits for each state of older bridge column are 0.5%, 1%, 2%, and 2.5% column drifts (Δ/L) for slight, moderate, extensive, and complete damage states, respectively.

The studied bridges are the single column reinforced concrete bridge that constructed since 1976. For this bridge type, the column displacement can reflect the damage level of the bridge. Then, the column displacement is selected to be an engineering demand parameter (EDP) in this study. According to the suggestion of Jeon et al. [26] for the studied bridges, the EDP has four limit states, i.e. slight, moderate, extensive, and complete damage states.

FHWA [34] suggests that the plastic rotational capacity of a member should be based on the governing limit state for that member. The governing limit state is the state that has the least plastic rotational (or plastic curvature) capacity. In addition, failure mechanism of bridge column can be divided into three types such as brittle failure (shear failure), semi-ductile failure (flexure to shear failure), and flexural failure as demonstrated in Fig. 10. Shear demands (V_m) of columns of studied bridges are estimated from the moment capacity of the cross-section of the bridge column that considers an interaction between axial force and bending moments in two axes. The estimated shear demands are compared to the evaluated shear capacities (V_i and V_f) of bridge column members in order to categorize the failure type of the studied bridges. The results are shown in Table 4. More details are shown in Chomchuen [37].

Table 4
Evaluation of failure type of the studied bridges by comparing shear demands with shear capacities of bridge column members.

	Bridge column height		
	4.5 m	6.3 m	15.0 m
Initial shear capacity (V_i) (kg)	382,483.1	361,768.2	338,731.9
Final shear capacity (V_f) (kg)	316,794.2	296,079.3	273,043
Shear demand (V_m) (kg)	412,877.5	296,423.6	124,664.5
Failure type	Brittle	Semi-ductile	Flexure

Table 5
Limit states of three studied bridges with failure mechanism consideration.

Damage states	Lateral displacement limit (cm) (column drift, Δ/L (%))		
	4.5 m column height	6.3 m column height	15.0 m column height
Slight	–	3.48 (0.5)	7.83 (0.5)
Moderate	–	6.97 (1.0)	15.67 (1.0)
Extensive	–	–	31.33 (2.0)
Complete	2.49 (0.48) (brittle shear failure)	12.75 (1.83) (semi-ductile failure)	39.16 (2.5) (flexural failure)

Table 4 shows that the capacity of the bridge with short column is limited by the shear failure. The bridge with medium column can deform into some plastic region as the semi-ductile limit. The failure type of bridge with tall column is the flexural failure, which the compressive strain of unconfined concrete reached ultimate value. The evaluated failure mechanisms of the studied bridges are considered together with the previously described limit states in this study. Therefore, the limits of each damage state that used in this study are summarized in Table 5.

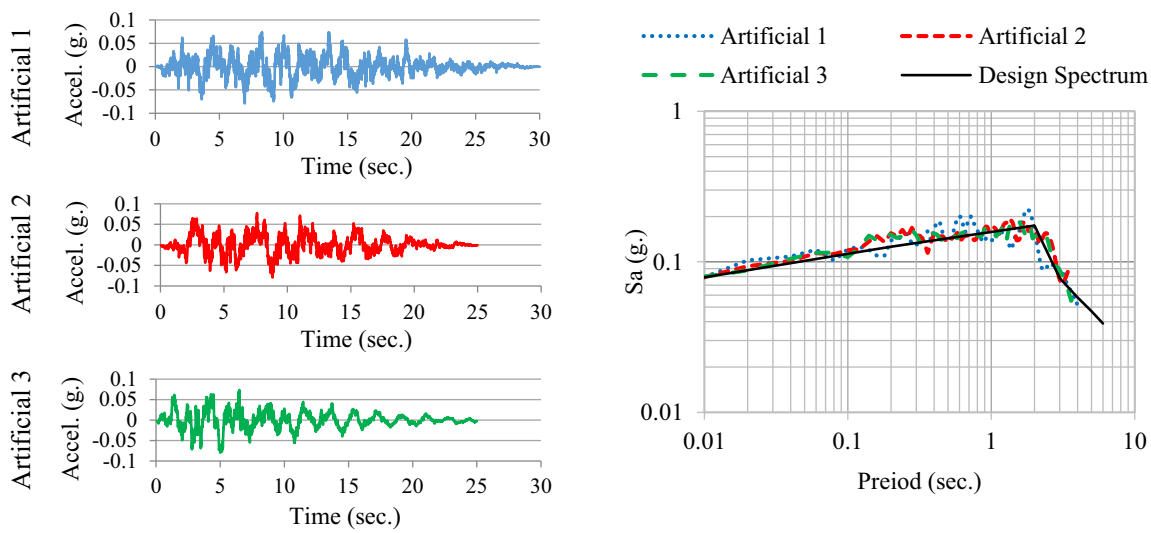

(a) Three artificial ground motions

(b) Comparison of response spectrum of generated ground motions with the design spectrum

Fig. 11. Artificial ground motions generated corresponding with the design spectrum for the inner area of Bangkok.

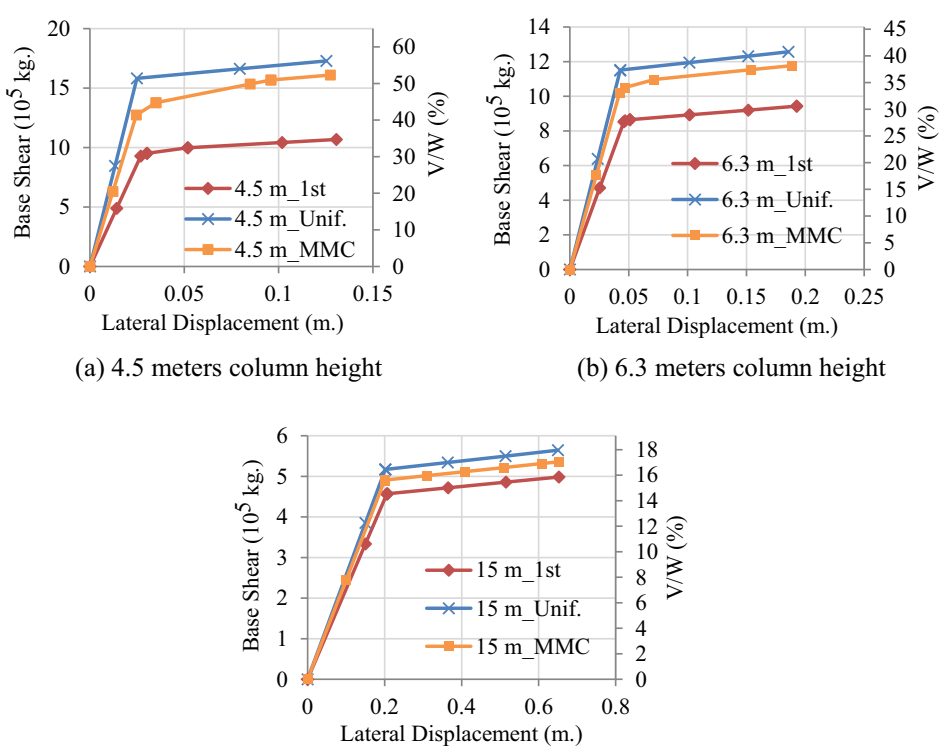

(a) 4.5 meters column height

(b) 6.3 meters column height

(c) 15.0 meters column height

Fig. 12. Lateral capacities of three studied bridges in transverse direction by NSA with three different load patterns.

The results in Table 5 mean that the studied bridge with short column collapses by brittle shear failure at only 0.48% drift. The studied bridge with medium column collapses by semi-ductile failure at 1.83% drift. The collapse of the studied bridge with tall column is controlled by the limit of complete damage state (2.5% drift). It should be noted that the estimation of capacity of the cross-section based on only the interaction of axial force and bidirectional moments leads to the flexural collapse limit exceeding 2.5% drift. This is because it did not automatically and directly consider the shear failure and column drift limitation.

4. Artificial ground motions

To evaluate the seismic performance of the bridge structures, the ground motion should be selected carefully because each ground motion form each earthquake has its own unique characteristic. According to the Seismic Retrofitting Manual for Highway Bridges published by the Federal Highway Administration [34], the maximum response of the three ground motions should be used for evaluating performance of structure. Therefore, this study uses the design spectrum for the inner area of Bangkok, Thailand [28] to be the target spectrum as shown in Fig. 11(b). The ground motions are generated by matching the response spectrum with the target spectrum. Three artificial ground motions generated by SeismoArtif [38] are referred as A1, A2, and A3 and shown in Fig. 11(a).

5. Nonlinear static analysis of the studied bridges with various load patterns

In order to evaluate seismic performance of the structures by the concept of IDA of ESDOF, the equivalent lateral behavior of ESDOF is firstly obtained from NSA of MDOF. Three selected lateral load patterns included proposed load pattern are applied to MDOF of the studied bridges. Then, NSA of MDOF of the studied bridges are performed. The results are shown in Fig. 12.

Fig. 12 also shows that using two different load patterns according to FEMA 356 gives strongly different lateral capacity and stiffness especially for the studied bridge with low first-mode participating mass ratio, i.e. bridge with short column in this study (Fig. 12(a)). The maximum base shear capacity of this bridge eval-

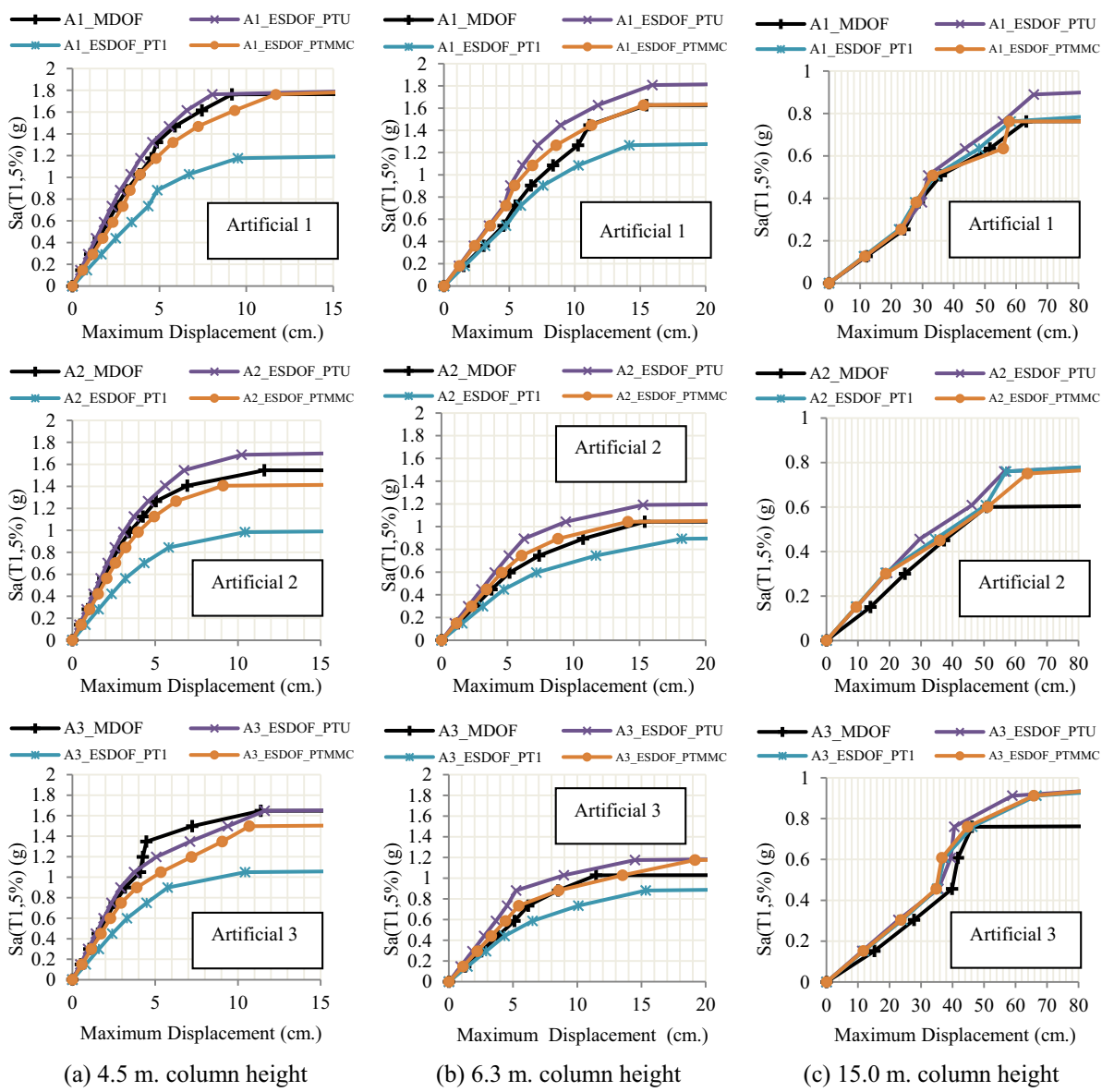

Fig. 13. Comparison of IDA curves of three studied bridges under three artificial ground motions obtained from NTHA of MDOF and ESDOF with three different lateral capacities in transverse direction.

uated by 1st is about 62% of those evaluated by Unif while MMC gives about 93% of those evaluated by Unif. For the studied bridge with medium column, the maximum capacity evaluated by 1st is about 75% of those evaluated by Unif while MMC gives about 94% of those evaluated by Unif. The maximum base shear capacity of the studied bridge with tall column evaluated by 1st is about 88% of those evaluated by Unif while MMC gives about 95% of those evaluated by Unif. Furthermore, the maximum capacity of the studied bridges with 4.5 m, 6.3 m, and 15 m column heights evaluated by MMC are 52.40%, 38.18%, and 17.06% of total weights, respectively, when the interaction of only force and bidirectional moments are considered. When additional shear failure and column drift are considered, the maximum base shear capacity of the studied bridges with 4.5 m, 6.3 m, and 15 m column heights evaluated by MMC are 41.43%, 36.81%, and 16.23% of total weights, respectively.

The following summations can be observed from Fig. 12 and Table 2. (1) The effect of different load pattern decreases when bridge column height or the first mode participating mass ratio of the bridge increases. (2) The proposed MMC load pattern results in the better accuracy of seismic capacity for all studied bridges. (3) The Unif load pattern leads to the upper bound result while the 1st yields the lower bound result.

6. Incremental dynamic analysis of studied bridges by ESDOF with various load patterns

IDA of the studied bridges by ESDOF with three considered load patterns under artificial ground motions are performed. Fig. 13(a)–(c) shows IDA curves of the studied bridges with 4.5 m, 6.3 m, and 15 m column heights, respectively. The IDA curve obtained from the ESDOF with lateral capacity from 1st, Unif, and MMC are referred as ESDOF_PT1, ESDOF_PTU, and ESDOF_PTMMC, respectively.

6.1. Effect of lateral load pattern on the IDA curves

The comparisons in Fig. 13(a)–(c) emphasize that the results of IDA of ESDOF significantly depend on selecting lateral load pattern. Effects of different lateral load patterns become more apparent when the bridge has low first-mode participating mass ratio (Table 2). The 1st mode load pattern leads to significantly under-estimate seismic capacity while Unif load pattern results in slightly over-estimate seismic capacity compared with the results from IDA of MDOF for the bridges with 4.5 m as shown in Fig. 13(a). The effects of load pattern become lower when first-mode participation mass ratio of the bridge increase as shown in Fig. 13(b) and (c) for bridges with 6.3 m and 15 m column heights, respectively. This response is similar to that of the buildings.

The results also reveal that the IDA curves obtained by ESDOF are essentially related to lateral capacity generated by NSA. This point implies that IDA curves obtained by ESDOF are significantly related to lateral load patterns. It should be noted that the different load patterns result in difference capacity and stiffness of ESDOF, as previously shown in Fig. 13. Therefore, although the ESDOFs have the same frequency and damping, the differences in capacity, mass, and stiffness of ESDOF result in different IDA curves. Therefore, the conclusions of IDA of ESDOF with various load patterns are the same as NSA with various load patterns.

6.2. Effect of hysteresis modeling on the IDA curves

6.2.1. Hysteresis modeling

Three built-in hysteresis models in SAP2000 are considered in this study. Kinematic model, pivot model, and Takeda model are shown in Fig. 14(a)–(c), respectively. The three considered models are used to model hysteresis behavior of ESDOFs in order to

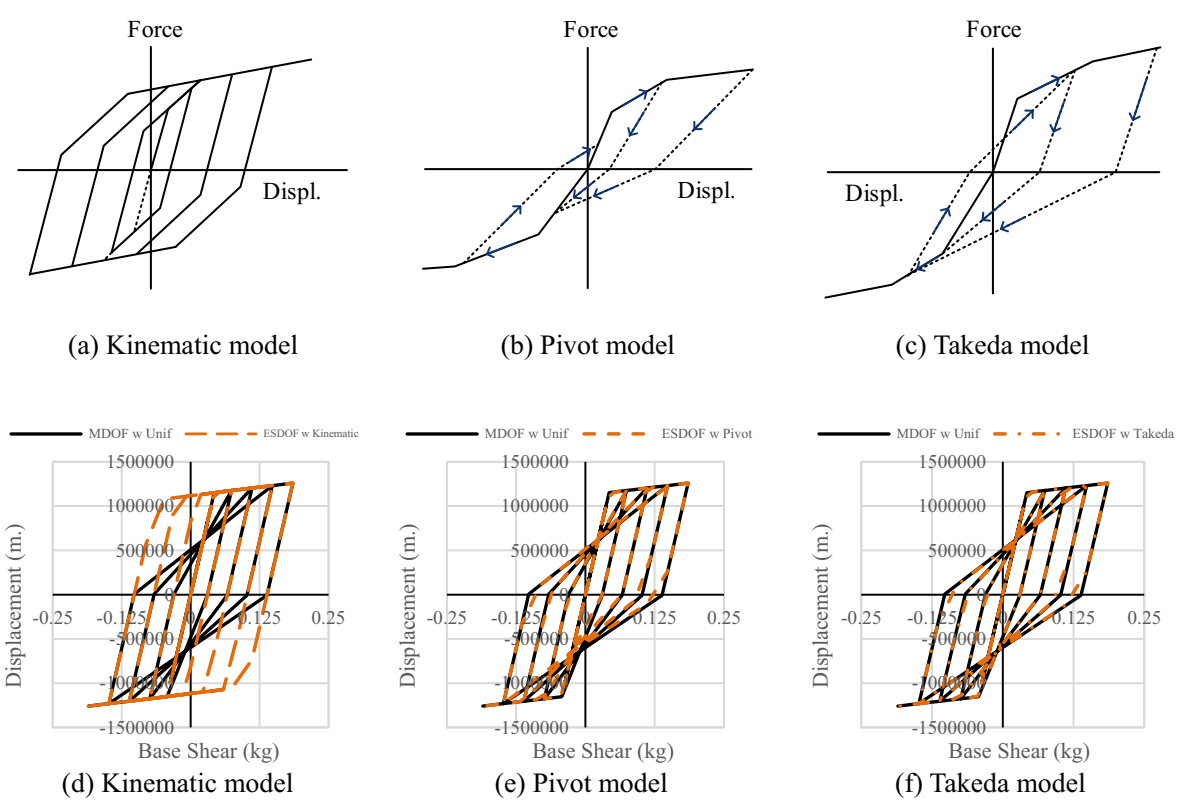

Fig. 14. Three different hysteresis models: (a–c) [25] and comparisons of cyclic lateral behavior of the studied bridge with 6.3 m column height obtained from CNSA of MDOF and CNSA of ESDOF with three different hysteresis models: (d–f).

observe their effects on the IDA curves of the studied bridges that generated by IDA of ESDOF.

The kinematic model is used for modeling hysteresis behavior without degrading hysteretic loop. The Takeda model is used for modeling hysteresis behavior with degrading hysteretic loop based on Takeda model. Both models are built-in function which all required parameters are automatically generated by the program. The pivot model is similar to the Takeda model, but additional parameters are required to control the degrading hysteretic loop. It is particularly well suited for reinforced concrete members, and is based on the observation that unloading and reverse loading tend to be directed toward specific points, called pivots points, in the force-deformation plane [33]. This study performs the cyclic nonlinear static analysis (CNSA) of MDOF to evaluate these parameters required for modeling the pivot model for all studied bridges.

Fig. 14(d)–(f) shows the comparisons between cyclic lateral behavior of the studied bridge with 6.3 m column height obtained from CNSA of MDOF and CNSA of ESDOF. It is shown that ESDOF with kinematic model results over-hysteretic loop while both ESDOF with pivot and Takeda models result accurate hysteretic loop compared with MDOF.

6.2.2. Comparison of IDA curves evaluated by IDA of ESDOF with three different hysteresis models

The IDA curves of three studied bridges generated from IDA of ESDOF with three different hysteresis models are compared with the IDA curves generated by IDA of MDOF. To conveniently observe the effects of different hysteresis models, the IDA curves of the studied bridges under A1 ground motion are shown in Fig. 15. By observing both shape and maximum capacity of IDA curves from Fig. 15, the IDA curves of ESDOF with kinematic model show significantly different maximum capacity compared with IDA of MDOF. While, the ESDOF with pivot model and Takeda model show more accurate results. However, the IDA curves of ESDOF with Takeda model agree well with IDA curves of MDOF only for the cases of bridge with short and medium column heights. The IDA curves of ESDOF with pivot model agree well with IDA curves of MDOF for all cases. Therefore, the IDA of ESDOF in this study will be performed by ESDOF with pivot model.

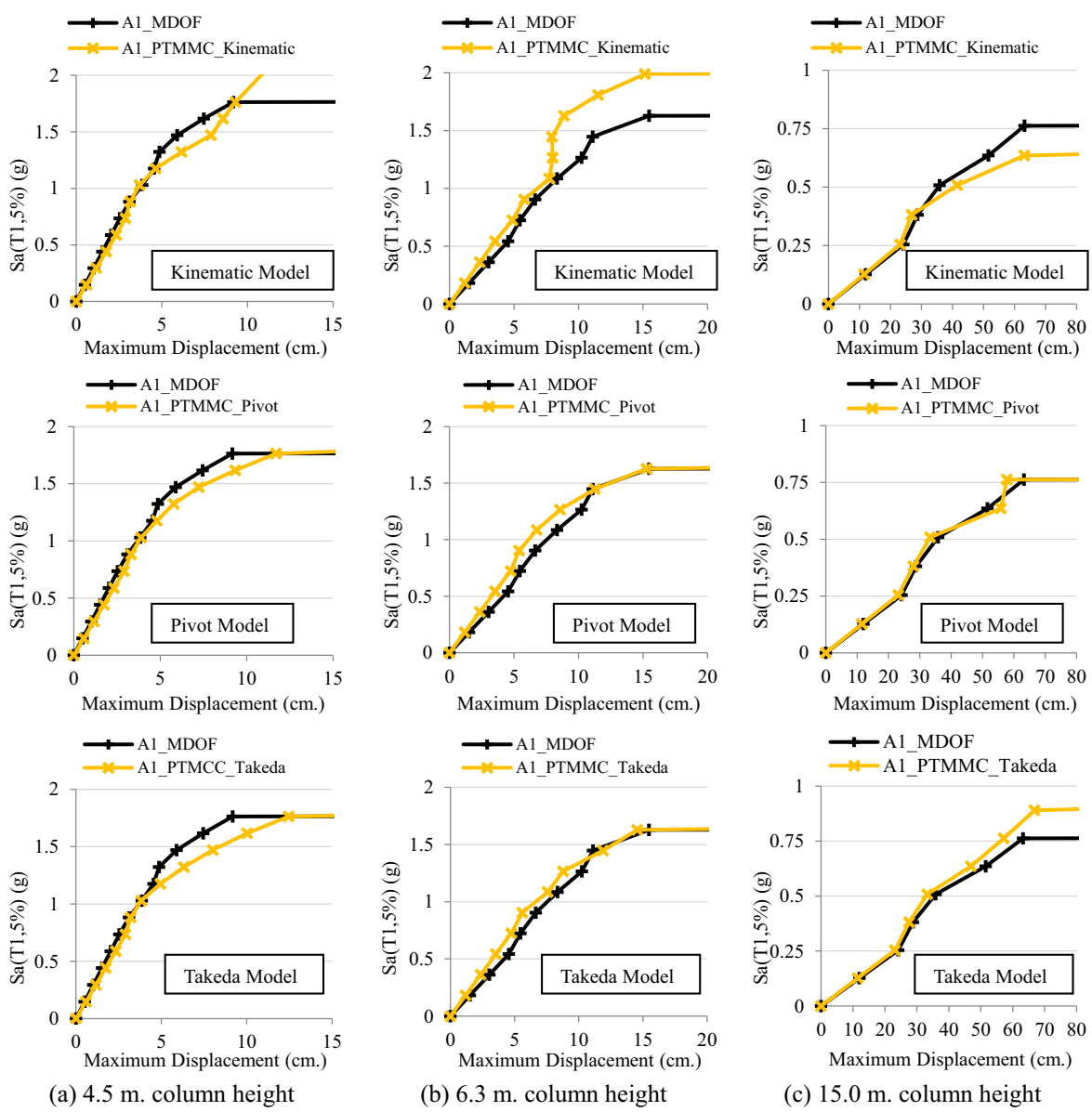

Fig. 15. Comparison of IDA curves of three studied bridges under A1 artificial ground motion generated by the IDA of ESDOF with three different hysteresis models.

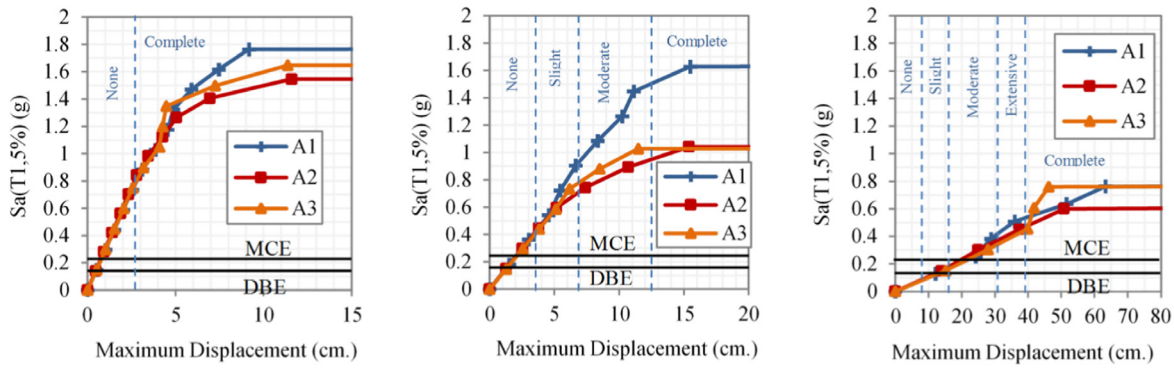

(a) 4.5 m. column height (b) 6.3 m. column height (c) 15.0 m. column height

Fig. 16. IDA curves of three studied bridges under three artificial ground motions generated by NTHA of MDOF.

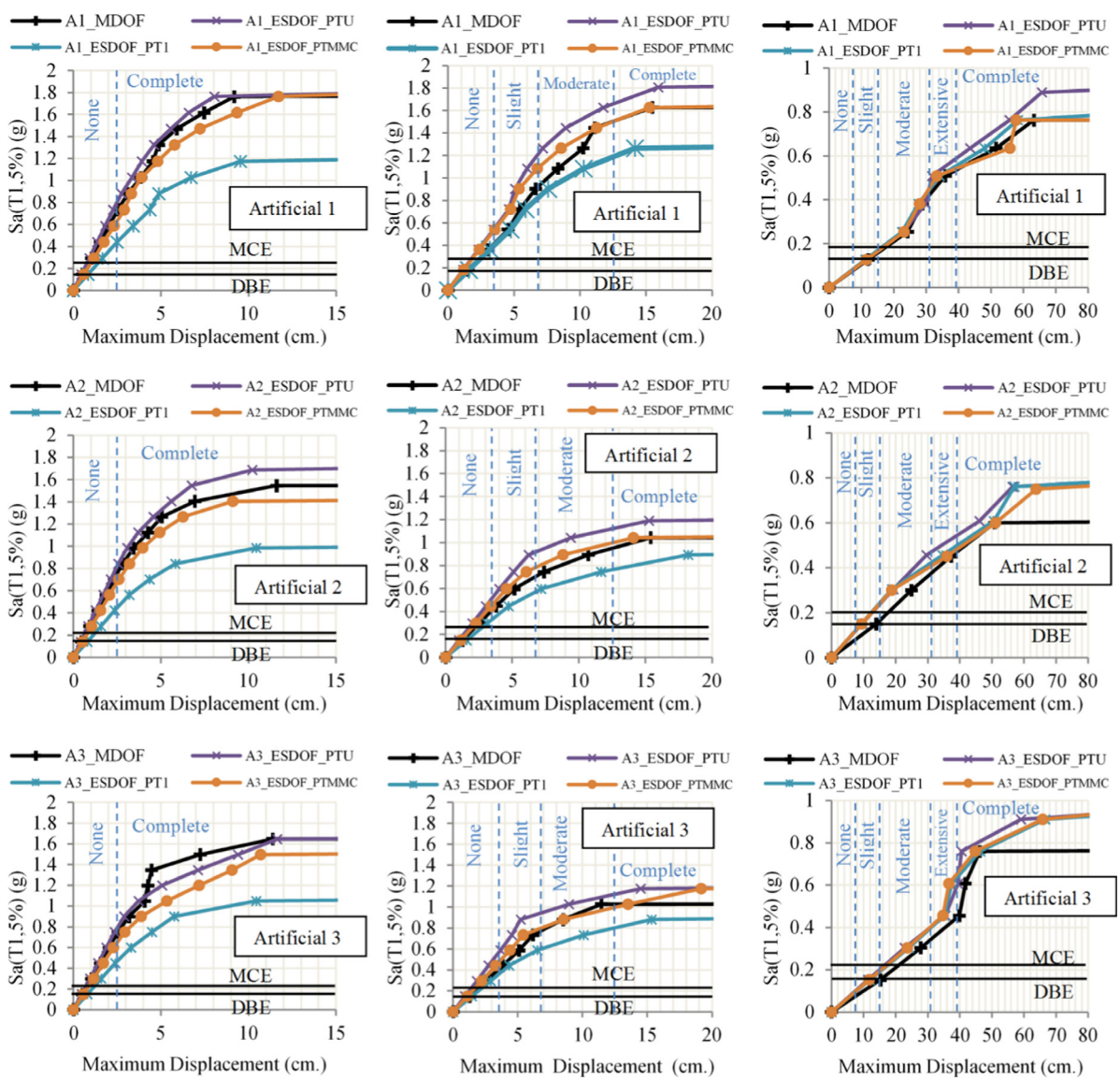

(a) 4.5 m. column height (b) 6.3 m. column height (c) 15.0 m. column height

Fig. 17. Performance level of three studied bridges under three artificial ground motions obtained from NTHA of MDOF and ESDOF with three different lateral capacities in transverse direction.

Table 6
Seismic performance levels of the three studied bridges under three artificial ground motions.

Bridges	Structural modeling method	Damage state					
		Design basis earthquake (DBE)			Maximum considered earthquake (MCE)		
		A1	A2	A3	A1	A2	A3
4.5 m	MDOF	DS1	DS1	DS1	DS1	DS1	DS1
	ESDOF_PT1	DS1	DS1	DS1	DS1	DS1	DS1
	ESDOF_PTU	DS1	DS1	DS1	DS1	DS1	DS1
	ESDOF_PTMMC	DS1	DS1	DS1	DS1	DS1	DS1
6.3 m	MDOF	DS1	DS1	DS1	DS1	DS1	DS1
	ESDOF_PT1	DS1	DS1	DS1	DS1	DS1	DS1
	ESDOF_PTU	DS1	DS1	DS1	DS1	DS1	DS1
	ESDOF_PTMMC	DS1	DS1	DS1	DS1	DS1	DS1
15.0 m	MDOF	DS2	DS2	DS2	DS3	DS3	DS3
	ESDOF_PT1	DS2	DS2	DS2	DS3	DS2	DS3
	ESDOF_PTU	DS2	DS2	DS2	DS3	DS2	DS3
	ESDOF_PTMMC	DS2	DS2	DS2	DS3	DS2	DS3

Note: DS1 = None, DS2 = Slight, DS3 = Moderate, DS4 = Extensive, and DS5 = Complete.

7. Performance of the bridges under considered earthquake

The damage limit-states defined previously in Section 3.4 were applied to the IDA curves in order to evaluate the seismic performance level of the bridges under both design basis earthquake (DBE) and maximum considered earthquake (MCE) for the inner area of Bangkok. According to the seismic design standard for the seismic risk regions in Thailand [20], the design spectrum for MCE can be selected and constructed depends on the area. Then, the design spectrum for MCE is reduced 1.5 times to be the design spectrum for DBE.

7.1. Evaluation by NTHA of MDOF model of bridges

In order to evaluate the seismic performance of the studied bridges, the damage limit-states are defined to the IDA curves obtained from IDA of MDOF of the bridges as shown in Fig. 16.

When compare with DBE and MCE for inner area of Bangkok in Figs. 11 and 16, the results show that no any damage occur for the bridges with 4.5 m and 6.3 m column heights. However, slight damage occurs for the bridge with 15 m column height under DBE while moderate damage occurs under MCE.

The results in Fig. 16 also show that the IMs of MDOF at collapse are 1.546 g, 1.028 g, and 0.600 g for the studied bridges with 4.5 m, 6.3 m, and 15 m column heights, respectively. These are corresponding to peak ground acceleration of 0.854 g, 0.543 g, and 0.310 g for bridge with 4.5 m, 6.3 m, and 15 m column heights, respectively.

7.2. Efficiency of ESDOF with various load patterns in evaluating the seismic performance of the bridges

To investigate the efficiency of ESDOF in evaluating the seismic performance of the bridges, the damage limit-states were applied to the IDA curves as shown in Fig. 17. The performance levels of the studied bridges evaluated from Fig. 17 are summarized in Table 6.

Table 6 shows that the studied bridges have no damage under the earthquake level for the inner area of Bangkok except bridge with 15 m column height as same as described in Section 7.1. It also shows that the ESDOF can be used efficiently for evaluating the seismic performance of the structures like the studied bridges under the low earthquake level. If the studied bridges situate in the moderate seismic zone, such as the northern area of Thailand, the different ESDOF may lead to the highly different of seismic performance level and suitable lateral load pattern should be seriously considered.

8. Conclusions

This study proposes the lateral load pattern that includes higher mode effect for single-run displacement-based NSA to evaluate the lateral behavior of ESDOF for performing IDA of ESDOF. The applicability of proposed load pattern is investigated through evaluating seismic performance of the studied bridges. The results lead to the following conclusions.

- The use of the concept of ESDOF for evaluating the seismic performance of the studied bridges by the mean of IDA can reduce the computational time from 60 min per load case for MDOF to 4 min per load case for ESDOF. That is a reduction of about 93% computational time. This is of high interest for risk analysis of bridge portfolios.
- The different load patterns result in difference capacity and stiffness of ESDOF. Therefore, although the ESDOFs have the same frequency and damping, the differences in capacity, mass, and stiffness of ESDOF result in different IDA curves. The ESDOF with the proposed multi-modes combination load pattern with single-run NSA and IDA gives better accuracy of seismic performance than the conventional load patterns for all studied bridges, compared with IDA of MDOF.
- Either the first mode or the uniform acceleration lateral load patterns based on FEMA 356 can be used effectively in applying the concept of ESDOF for evaluating the seismic performance of the studied bridge that have the first-mode participating mass ratio higher than 80% of the total mass, i.e. the case for the 15 m column height in this study.
- For the seismic performance of studied bridges with the first-mode participating mass ratio less than 80% of the total mass, i.e. 4.5 m and 6.3 m column heights in this study, the ESDOF with the first mode load pattern leads to moderately underestimate capacities while the uniform acceleration results in slightly over-estimate capacities.
- The studied bridge with short and medium column height collapse as brittle shear failure and semi-ductile failure when the shear failure criteria was considered. In other words, evaluating seismic performance of studied bridges by IDA without consideration of shear failure and column drift limit result in moderately to significantly over-estimated capacity of the bridges with short and medium column height.

- The IDA curves of ESDOF with kinematic model show significantly different maximum capacity compared with IDA of MDOF. While, the ESDOF with pivot model and Takeda model show more accurate results. The ESDOF with pivot hysteresis model shows the most accurate IDA curves with IDA of MDOF in this study. However, the required input parameters to model the pivot hysteresis must be extracted from the results of cyclic nonlinear static analysis. The ESDOF with Takeda hysteresis model results slightly less accurate IDA curves than those of ESDOF with pivot hysteresis model compared with IDA of MDOF. However, the necessary parameters for modeling Takeda hysteresis are automatically generated by the program.
- The IMs in term of spectrum acceleration of MDOF at collapse are 1.546 g, 1.028 g, and 0.600 g for the studied bridges with 4.5 m, 6.3 m, and 15 m column heights, respectively. These are corresponding to peak ground acceleration of 0.854 g, 0.543 g, and 0.310 g for bridge with 4.5 m, 6.3 m, and 15 m column heights, respectively.

Acknowledgments

The research described in this paper was financially supported by the Thailand Research Fund (TRF) under the Royal Golden Jubilee Ph.D. Program contract number PHD/0296/2549 and by the Higher Education Research Promotion and National Research University Project of Thailand, Office of the Higher Education Commission.

References

[1] Vamvatsikos D, Cornell CA. Incremental dynamic analysis. Earthquake Eng Struct Dynam 2002;31(3):491–514.
[2] Mander JB, Dhakal RP, Mashiko N, Solberg KM. Incremental dynamic analysis applied to seismic financial risk assessment of bridges. Eng Struct 2007;29(10):2662–72.
[3] Vejdani-Noghreiyan HR, Shooshtari A. Comparison of exact IDA and approximate MPA-based IDA for reinforced concrete frames. In: Proceedings of the 14th world conference on earthquake engineering, Beijing, October; 2008.
[4] Tehrani P, Mitchell D. Seismic performance assessment of bridges in Montreal using incremental dynamic analysis. In: Proceedings of the 15th world conference on earthquake engineering, Lisbon, September; 2012.
[5] Tehrani P, Mitchell D. Seismic response of bridges subjected to different earthquake types using IDA. J Earthquake Eng 2013;17(3):423–48.
[6] Alembagheri M, Ghaemian M. Damage assessment of a concrete arch dam through nonlinear incremental dynamic analysis. Soil Dynam Earthquake Eng 2013;44(1):127–37.
[7] Nazari YR, Bargi Kh. Seismic performance assessment of a two span bridge by applying incremental dynamic analysis. Asian J Civ Eng 2014;15(1):1–8.
[8] Elnashai AS, Di Sarno L. Fundamentals of earthquake engineering. UK: Wiley and Sons; 2015.
[9] Vamvatsikos D, Cornel CA. Seismic performance, capacity and reliability of structures as seen through incremental dynamic analysis. Report no. 151; 2005.
[10] Federal Emergency Management Agency (FEMA). Effects of strength and stiffness degradation on seismic response (FEMA P440A), Redwood City, CA, USA; 2009.
[11] Mofid M, Zarfam P, Fard BR. On the modal incremental dynamic analysis. Struct Des Tall Spec Build 2005;14(4):315–29.
[12] Han SW, Chopra AK. Approximate incremental dynamic analysis using modal pushover analysis procedure. Earthquake Eng Struct Dynam 2006;35(2):1853–73.
[13] Han SW, Moon KH, Chopra AK. Application of MPA to estimate probability of collapse of structures. Earthquake Eng Struct Dynam 2010;39(11):1259–78.
[14] Zarfam P, Mofid M. On the modal incremental dynamic analysis of reinforced concrete structures, using a trilinear idealization model. Eng Struct 2011;33(4):1117–22.
[15] Chopra AK, Goel RK. A modal pushover analysis procedure to estimate seismic demands for buildings (PEER2001/03). Pacific Earthquake Engineering Research Center, University of California Berkeley; 2001.
[16] Hernadez-Montes E, Kwon OS, Aschheim MA. An energy-based formulation for first- and multiple-mode nonlinear static (pushover) analysis. J Earthquake Eng 2004;8(1):69–88.
[17] Antoniou S, Pinho R. Advantages and limitations of adaptive and non-adaptive force-based pushover procedures. J Earthquake Eng 2004;8(4):497–522.
[18] Kunnath SK. Identification of modal combinations for nonlinear static analysis of building structures. Comput-Aid Civ Infrastruct Eng 2004;19(4):282–95.
[19] Del Vecchio C, Kwon OS, Di Sarno L, Prota A. Accuracy of nonlinear static procedures for the seismic assessment of shear critical structures. Earthquake Eng Struct Dynam 2015;44(10):1581–660.
[20] Lu Zhihao, Ge Hanbin, Usami T. Applicability of pushover analysis-based seismic performance evaluation procedure for steel arch bridges. Eng Struct 2004;26(13):1957–77.
[21] Bignell JL, LaFave JM, Hawkins NM. Seismic vulnerability assessment of wall pier supported highway bridges using nonlinear pushover analyses. Eng Struct 2005;27(14):2044–63.
[22] Saadeghvaziri MA, Yazdani-Motlagh AR. Seismic behavior and capacity/demand analyses of three multi-span simply supported bridges. Eng Struct 2008;30(1):54–66.
[23] Mwafy A, Kwon OS, Elnashai A. Seismic assessment of an existing non-seismically designed major bridge-abutment–foundation system. Eng Struct 2010;32(8):2192–209.
[24] Bassam A, Iranmanesh A, Ansari F. A simple quantitative approach for post earthquake damage assessment of flexure dominant reinforced concrete bridges. Eng Struct 2011;33(12):3218–25.
[25] Camara A, Astiz MA. Pushover analysis for the seismic response prediction of cable-stayed bridges under multi-directional excitation. Eng Struct 2012;41(1):444–55.
[26] Jeon JS, Shafieezadeh A, Lee DH, Choi E, DesRoches R. Damage assessment of older highway bridges subjected to three-dimensional ground motions: characterization of shear–axial force interaction on seismic fragilities. Eng Struct 2015;85(1):47–57.
[27] Kitagawa Y, Hiraishi H. Overview of the 1995 Hyogo-ken Nanbu earthquake and proposal for earthquake mitigation measures. J Jpn Assoc Earthquake Eng 2004;4(Special issue):1–29.
[28] Department of Public Works and Town & Country Planning (DPT). Seismic resistance design standard (DPT-1302-52), Bangkok, Thailand; 2009 [in Thai].
[29] Aviram A, Mackie KR, Stojadinovic B. Guidelines for nonlinear analysis of bridge structures in California (PEER2008/03). Pacific Earthquake Engineering Research Center, University of California Berkeley; 2008.
[30] Yazdani N, Eddy S, Cai CS. Effect of bearing pads on precast prestressed concrete bridges. J Bridge Eng 2000;5(3):224–32.
[31] Thammasat University Research and Consultancy Institute (TU-RAC). Inspection and methodology for replacing bearing pads of expressway in Thailand, Pathumthani, Thailand; 2007 [in Thai].
[32] American Association of State Highway and Transportation Officials (AASHTO). LRFD bridge design specifications, 5th ed. Washington, DC, USA; 2010.
[33] Computers & Structures (CSI). SAP2000 analysis reference, Berkeley, CA, USA; 2011.
[34] Federal Highway Administration (FHWA). Seismic retrofitting manual for highway structures: part 1 – bridges, Buffalo, NY, USA; 2006.
[35] Federal Emergency Management Agency (FEMA). Prestandard and commentary for the seismic rehabilitation of buildings (FEMA 356), Washington, DC, USA; 2000.
[36] Hazus. Hazus-MH 2.1 technical manual, Washington, DC, USA; 2003.
[37] Chomchuen P. Seismic performance evaluation and improvement of regular reinforced concrete bridges. PhD dissertation. Thammasat University, Pathumthani, Thailand; 2015.
[38] http://www.seismosoft.com/seismoartif.